water

MDPI

Article

Removing Norfloxacin from Aqueous Solutions Using Biochar Derived from Waste Disposable Bamboo Chopsticks

Ming Zhang [1,2], Shuai Shao [1], Penghui Li [1] and Runjuan Zhou [1,*]

[1] School of Chemical and Environmental Engineering, Anhui Polytechnic University, Wuhu 241000, China; zhangming@ahpu.edu.cn (M.Z.); shaoshuai19971107@163.com (S.S.); 15556354182@163.com (P.L.)
[2] Anhui Engineering Research Center of Green Building and Digital Construction, Wuhu 241000, China
* Correspondence: rjzhou@126.com

Abstract: The presence of antibiotics in water environments increases the resistance of bacterial and can also cause irreversible damage to ecosystems and the human body. In this study, disposable bamboo chopsticks were used as raw material to prepare bamboo biochar (BB) via oxygen-limited pyrolysis to remove norfloxacin (NOR) from aqueous solutions. The properties of the BB were explained through the characterization of its SBET, morphology, structure, and functional groups. The effects of the dosage, pH, ionic strength, and water type on the removal of NOR using BB were investigated. The maximum theoretical adsorption capacities (Q_{max}) of NOR removed by BB at 25, 35, and 45 °C obtained using the Langmuir model were 76.17, 77.22, and 105.19 mg/g, respectively. To facilitate a comparison with other types of biochar, this study also prepared biochar of rice straw, wheat straw, soybean straw, corn straw, rape straw, peanut shell, *Eichhornia crassipes*, and other biomass raw materials under the same preparation conditions as the BB. The results demonstrated that the removal rate of NOR using BB was the highest under the same adsorption conditions, reaching 99.71%. Biochar from waste disposable bamboo chopsticks can be used for the treatment of new types of pollutants in water bodies, such as antibiotics and other organic contaminants, which will help to achieve sustainable solid waste management.

Keywords: waste disposable; bamboo-based biochar; antibiotics; norfloxacin adsorption; sustainable waste resource utilization

Citation: Zhang, M.; Shao, S.; Li, P.; Zhou, R. Removing Norfloxacin from Aqueous Solutions Using Biochar Derived from Waste Disposable Bamboo Chopsticks. *Water* **2023**, *15*, 4306. https://doi.org/10.3390/w15244306

Academic Editors: Andreas Angelakis, Yiting Luo and Rongkui Su

Received: 5 November 2023
Revised: 4 December 2023
Accepted: 13 December 2023
Published: 18 December 2023

1. Introduction

Antibiotics, as broad-spectrum antibacterial agents, have long served in the human, livestock, and poultry medical industries. As a result, many antibiotics have been detected in productive waters and aquatic environments [1,2]. Norfloxacin (NOR) is a third-generation fluoroquinolone drug. Because of its good pharmacokinetics performance, wide antibacterial spectrum, strong antibacterial performance, and slight side effects, it can be used in combination with other antibiotics without cross-infection and has been widely used in the fields of medicine and aquaculture, among others [3]. NOR has a strong polarity and high water solubility. When at a low pH, NOR exists mainly in a cationic form, while at a neutral pH, NOR exists in a zwitterionic form. After NOR enters the human body, only about 40% of it is adsorbed, while about 60% remains unchanged and is excreted directly through the body into the environment [4]. Currently, NOR concentrations have been measured in water bodies ranging from ng^{-1} to μg^{-1}. The continued input of NOR into the environment may be harmful to aquatic life, humans, and wildlife. Even if concentrations are less than 0.5 mg/L, NOR temporarily reduces the stability of planktonic ecosystems and affects interactions among species [5]. The presence of low concentrations of NOR in ecosystems presents a major threat to indigenous microorganisms [6]. Therefore, it is imperative to develop environmentally friendly, efficient, and cost-effective treatment methods to remove residual NOR from water bodies. At present, the common physical

and chemical treatment methods for NOR and other antibiotics include membrane filtration [7,8], advanced oxidation [9,10], and adsorption [11,12]. Compared to the other two methods, the adsorption method has the advantages of being economically feasible, easily carried out, and environmentally friendly [13,14]. The adsorbent used is a major factor that affects the process of adsorption. Currently, some of the more advanced materials, including graphite oxides, covalent organic frameworks, and metal–organic frameworks, have played a significant role in adsorbing antibiotics [15–17]. However, the high cost of the aforementioned materials, added to the fact that the media required to synthesize them are often poisonous and combustible, poses latent hazards to the ecosystem, thus restricting their use [18].

Over the past few years, biomass-derived biochar has become an economical and sustainable carbon-enriched material that can be used to remove residual antibiotics from the environment. Biochar is generally prepared from wood, agricultural/forest waste, fruit by-products, and other carbon-rich biomass materials under mild pyrolysis conditions [19]. Compared to other biomass-derived biochars, bamboo biochar has the characteristic of high porosity, and its raw materials are extensively planted in the Asia-Pacific region, so it has a great potential for application in these regions [20,21].

Disposable bamboo chopsticks are composed of bamboo, one of the fastest-growing plants on the Earth and a highly productive renewable resource. Because disposable bamboo chopsticks are very economical and hygienic, they are widely used in the catering industry. With the development of China's take-out industry in recent years, the use of disposable tableware has increased dramatically, resulting in a large amount of solid waste. This has hindered achieving the goal of the "reduction of pollution and carbon emissions" and the construction of "waste-free cities", so the recycling of disposable bamboo chopsticks is a problem that needs an urgent solution. Previous studies have reported that bamboo-based biochar (BB) was applied to Mn, methylene blue dye (MB), and sulfamethoxazole adsorption [22–24].

In this work, bamboo biochar (BB) was prepared from disposable bamboo chopsticks to adsorb NOR in aqueous solutions. The influence of the thermolysis temperature, dosage, and solution pH on the adsorption of NOR using bamboo biochar was investigated. Subsequently, the adsorption isotherms and kinetics of NOR on biochar were investigated to explore the adsorption mechanism. At the same time, experiments with different ionic strengths and types of water were intended to investigate the adsorption property of the disposable bamboo chopstick biochar for NOR. The NOR adsorption performance of the waste disposable bamboo chopstick biochar was compared with that of other types of biomass-derived biochar under the same preparation conditions. The aims of this study are as follows: firstly, to establish a universal method for fabricating adsorbents from waste disposable bamboo chopsticks, specifically for controlling antibiotic pollution, and secondly, to elucidate the mechanism of NOR removal using biochar through a combination of adsorption experiments and characterization techniques. This research also contributes to the recycling of waste resources, offering a practical approach toward the overarching objective of "reducing pollution and carbon emissions".

2. Materials and Methods

2.1. Chemical Reagents

A stock solution of 200 mg/L norfloxacin (NOR) ($C_{16}H_{18}FN_3O_3$, 99.5%) was created by dissolving 0.2 g NOR in 1 L of ultrapure water. The various concentrations of norfloxacin solutions used in the experiments were diluted from the stock solutions, and 0.1 mol/L NaOH or 0.1 mol/L HCl solutions were utilized to adjust the pH value of all solutions. Ultrapure water was utilized to prepare the solutions for all experiments. All reagents used throughout this work were analytically pure and purchased from Sinopharm Chemical Reagent Co., Ltd., Shanghai, China.

2.2. Preparation of BB

The waste disposable bamboo chopsticks (WDBCs) in this study were gathered in the canteen of Anhui Polytechnic University. The collected WDBCs were firstly washed in warm water with detergent for cleaning, and the surface was cleaned of oil and then sprinkled with the tap water. Secondly, the WDBCs were washed numerous times with ultrapure water and dried in an oven at 80 °C for 24 h. Following that, a grinder was employed to pulverize the dried WDBCs into powder, which was then sifted using a 60-mesh screen to prepare the biochar precursor. Then, 10 g of the dry WDBCs was placed in a muffle furnace for pyrolysis under the following pyrolysis conditions: 300, 500, 600, 700, and 800 °C for 2 h (heating rate of 5 °C/min). To salvage energy during the pyrolysis process, the crucible cup was sealed with aluminum foil instead of nitrogen atmosphere to isolate the oxygen. At the end of the pyrolysis, the biochar was naturally cooled to room temperature and then removed from the muffle furnace. The biochar exhibited a grayish-white top layer and a black bottom layer; it was ground in a 100-mesh sieve and kept in the sealed reagent bottle before being utilized in further experiments.

2.3. Adsorption Experiments

The adsorption experiments were conducted in 50 mL polyethylene centrifugal tubes. A predetermined amount of BB was weighted and scattered in a 20 mL NOR solution. The solutions were stirred at 150 rpm/min at 25 °C in a water bath oscillator, SHA-CA (Jingda Instrument Co., Ltd., Changzhou, China). In the effect-of-pyrolysis temperature experiments, a NOR concentration of 10 mg/L, pH of 6.0, and BB of 0.75 g/L were used. In the dosage influence experiments, a dose range of 0.1–2.0 g/L, a NOR concentration of 20 mg/L, and a pH of 6.0 were selected. In the initial pH effect experiments, the pH of solutions ranged from 2.0 to 10, the concentration of NOR was 20 mg/L, and a BB dosage of 2.0 g/L was chosen.

To evaluate the influence of ionic strength on NOR adsorption, the experimental conditions were the following: a concentration of NOR at 20 mg/L, a dose of BB at 2.0 g/L, pH of 6.0, and the reaction volume of the solution was 20 mL. The concentration range of NaCl and $CaCl_2$ solutions was from 0 to 1.0 mol/L. The ultrapure water, tap water, and river water were used only for the application tests. Among the three solutions, the sample of river water was drawn from the river located near Anhui Polytechnic University. Then, 0.45 μm syringe filters were utilized to remove the suspended matter in the river water samples. Other operating conditions were the same as in the ionic strength impact experiments.

Kinetic and isotherm experiments were utilized to investigate the adsorption behavior of BB. In the kinetic experiments, a BB dosage of 2.0 g, NOR concentration of 20 mg/L, pH of 6.0, and solution volume of 1000 mL were used. Samples were sampled at 10, 30, 60, 90, 120, 150, 180, 210, and 240 min. In the isotherm experiments, the NOR concentrations ranged from 10 to 300 mg/L, with a solution volume of 20 mL, dosage of 2.0 g/L, reaction time of 240 min, and pH of 6.0. The kinetic experimental data were fitted by the pseudo-first-order and pseudo-second-order models, both of which are contained in Equations (1) and (2), and the Langmuir and Freundlich models were applied to analyze the equilibrium data. The models are expressed as follows in Equations (3) and (4) [25]:

$$q_t = q_e(1 - \exp(-k_1 t)) \quad (1)$$

$$q_t = \frac{q_e^2 k_2 t}{1 + q_e k_2 t} \quad (2)$$

$$q_e = \frac{K_a Q_{max} C_e}{1 + K_a C_e} \quad (3)$$

$$q_e = K_F C_e^{\frac{1}{n}} \quad (4)$$

In Equations (1) and (2), q_e (mg/g) is the adsorption capacity at the moment of equilibrium, and q_t (mg/g) is the adsorption capacity at time t (min). k_1 (min^{-1}) and k_2 (g/mg·min) are constants of the pseudo-first-order and the pseudo-second-order models, respectively. In Equations (3) and (4), C_e (mg/L) is the equilibrium concentration of the solution. K_a and K_F are constants for the Langmuir and the Freundlich models, respectively. Q_{max} is the maximum theoretical adsorption capacity (mg/g) obtained from Langmuir model fitting (mg/g). n (Freundlich index) is the index of intensity change and adsorption deviation during adsorption.

For NOR analysis, samples were separated by a 0.45 μm syringe filter, and the concentration of NOR was measured by the UV-VIS spectrophotometer (Shimadzu Co., Ltd., Tokyo, Japan) at a wavelength 300 nm. All experiments were conducted in triplicate and the experimental data were compiled as the average of the three experiments. Except for the adsorption kinetic experiments, all the additional experiments reacted for 300 min.

2.4. Characterization of BB

The specific surface area and particle size of BB were determined by the Brunauer–Emmett–Teller method (BET, NOVA 2000e, Quantachrome Instruments, Boynton Beach, FL, USA) via N_2 adsorption–desorption isotherm at 77 K. The morphological characteristics of BB were observed by SEM (S-4800, Hitachi Ltd., Tokyo, Japan). The samples were spread in ethanol on a sample stage and subsequently coated with a layer of gold using sputtering. The functional groups of BB were determined by a Fourier-transform infrared spectroscopy spectrometer (FTIR, IRPrestige-21, Shimadzu Co., Ltd., Tokyo, Japan), with a measured range from 400 to 4000 cm^{-1}. The crystal structure of BB was analyzed by X-ray diffraction (XRD, D8, Bruker Co., Karlsruhe, Germany). The pH of BB was determined by a pH meter (PHS25, LEICI, Shanghai, China), and the zero-point charge of biochar (pH_{pzc}) was obtained by pH drift experiments.

3. Results and Discussion

3.1. Effect of Pyrolysis Temperature on the NOR Adsorption by BB

The effects of the pyrolysis temperature on the NOR adsorption by the BB are displayed in Figure 1. The NOR adsorption efficiency of the BB increased with an increasing pyrolysis temperature. The results indicated that the BB prepared at 700 and 800 °C showed a better adsorption effect on NOR. When the dosage was 0.75 g/L, the NOR adsorption rate of BB-700 reached 99.71%. In contrast, BB-300, BB-500, and BB-600 removed only 28.11%, 46.14%, and 48.01% of the NOR, respectively. This may be explained by the lower pyrolysis temperature; the graphitization of biomass is low, limiting the ability of BB to adsorb the NOR by π–π interactions [2]. Moreover, because of the low temperature, incomplete decomposition of the organic matter leads to incomplete pore structure formation, resulting in a negligible specific surface area and providing fewer adsorption sites [26,27].

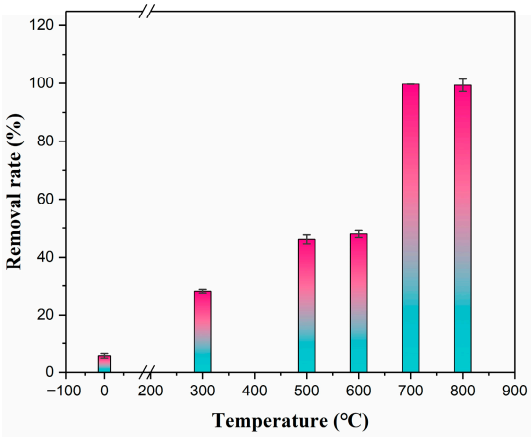

Figure 1. Effect of pyrolysis temperature on the ability of BB to remove NOR.

To verify the influence of the pyrolysis temperature on the NOR adsorption performance of BB, the SBET of raw biomass and BB prepared at different temperatures were measured, and the results are shown in Table 1. Based on the analysis of the SBET consequences, the specific surface areas of the BB at 700 and 800 °C were 576.76 and 574.70 m^2/g, respectively, which were 208.82 and 208.07 times the specific surface area of the raw biomass, respectively. In addition, the surface areas of the BB at 700 and 800 °C were bigger than the BB at other pyrolysis temperatures, which may be the reason for the better adsorption performance of BB at 700 and 800 °C. Compared to the untreated raw biomass, BB-700 and BB-800 have a smaller average pore diameter. On the contrary, the pore volumes of BB-700 and BB-800 are larger than those of the raw biomass and other BBs, indicating that the increased porosities were dominated by micropores [2]. Mesopores are conducive to the migration of antibiotics from the solution and pore filling, while micropores enable more adsorption pores for antibiotics, thus improving the adsorption performance of biochar [4], which means that BB-700 and BB-800 can be used as potential antibiotic adsorbents. After comprehensive consideration of its removal efficiency and economic benefits, BB-700 was chosen for subsequent experiments.

Table 1. Parameters of the SBET of raw biomass and BBs.

Samples	Specific Surface Area (m^2/g)	Pore Volume (cm^3/g)	Pore Diameter (nm)
Raw biomass	2.76	0.012	4.695
BB-300	18.97	0.003	3.703
BB-500	52.83	0.003	6.159
BB-600	278.01	0.029	3.326
BB-700	576.76	0.042	3.748
BB-800	574.70	0.099	3.735

3.2. Effect of Dosage and pH on the Performance of BB-700 for NOR Adsorption

The NOR removal rates by BB-700 under different dosages are shown in Figure 2. As depicted in Figure 2, the removal of NOR by BB-700 gradually increased with the increase in the dosage. When the dosage was raised from 0.1 to 2.0 g/L, the removal of NOR by BB-700 improved from 43.29% to 82.98%. When the dose was lower than 1.0 g/L, the adsorption points of BB-700 were too few to adsorb more NOR. The removal of NOR by BB-700 increased when the dose exceeded 1.0 g/L, possibly because, when the dosage increased, the adsorption sites increased, and there were enough sites to accommodate more NOR. Considering both the removal efficiency and economic cost, the dosage of BB-700 was 2.0 g/L in the subsequent experiments.

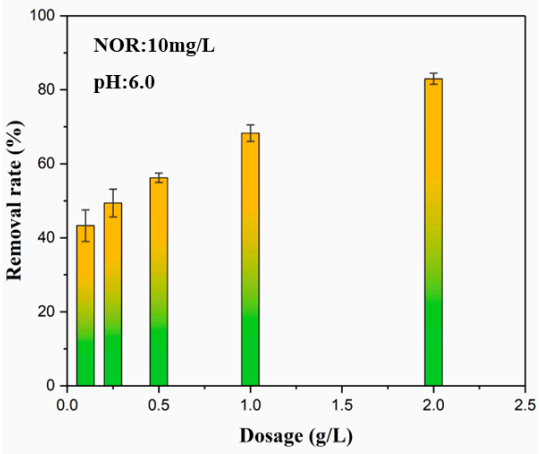

Figure 2. Effect of dosage on the adsorption performance of BB-700.

The influence of pHs in the range of 2–10 on the adsorption of NOR by BB-700 was investigated. As seen in Figure 3, the removal of NOR by BB-700 increased from 75.93% to 83.87% as the pH increased from 2 to 6, whereas the removal of NOR decreased significantly as the pH increased from 7 to 10. Differences in the pH of the adsorbent solution may cause protonation of the functional groups of biochar as well as changes in its surface charge [28]. Acidic conditions tend to promote the formation of hydrogen bonds, indicating that electrostatic attraction is not the main mechanism for NOR adsorption on biochar.

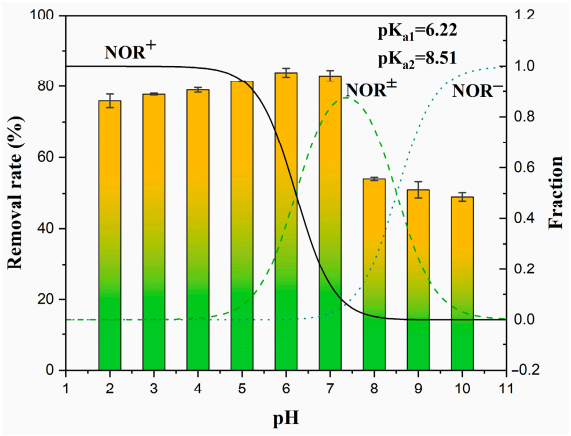

Figure 3. Effect of pH on the adsorption performance of BB-700.

NOR is reported to have two types of pK_a (6.22 and 8.51); therefore, under different pH conditions, NOR can exist in different ionic forms: cationic (pH < 6.22), zwitterionic (6.22 < pH < 8.51), and anionic (pH > 8.51) [29]. With a pH in the range of 2–6, the surface of BB-700 was charged positively, and the concentration of cationic NOR decreased with an increasing pH, thus reducing the electrostatic repulsion between BB-700 and the NOR and improving the efficiency of the removal of NOR. As the pH of the solution continued to increase, the removal of NOR by BB-700 decreased. As shown in Figure 4, the pH_{pzc} of BB-700 was 8.48, indicating that, when the pH < 8.48, BB-700 had a positive surface charge, and when the pH > 8.48, it was negative. Therefore, the reduced adsorption performance of BB-700 on NOR at pH < 6 and pH > 8 may be owing to the electrostatic repulsion between BB-700 and ionic NOR.

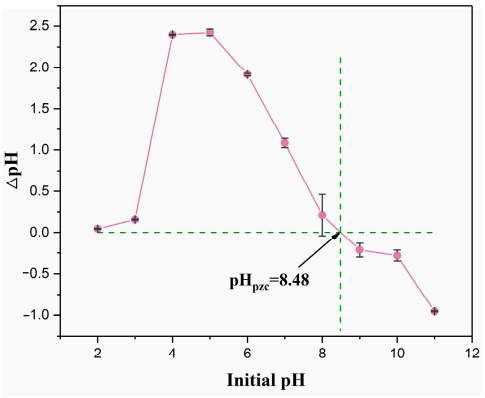

Figure 4. pH_{pzc} of BB-700.

3.3. Adsorption Isotherm and Kinetics Studies

Adsorption isothermal modeling can be applied to analyze the reaction that occurs between BB-700 and NOR as well as the properties of the adsorbed layer [30]. The adsorption isotherm experiment was performed at 25, 35, and 45 °C for different concentrations of NOR. The Langmuir and Freundlich model fit curves are shown in Figure 5, and the fitting parameters are displayed in Table 2. It can be seen from Figure 5 that, under the three

operating temperatures, the adsorption capacity of BB-700 for NOR increased rapidly when the concentration of NOR was low. However, as the NOR concentration increased, the adsorption capacity increased slowly, which was attributed to the fact that a finite number of active pores on the BB-700 surface were occupied by NOR at higher initial concentrations.

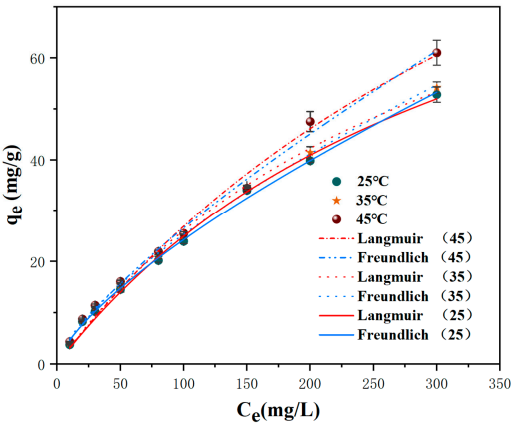

Figure 5. The experimental data and the fitted curves of the isotherm (Langmuir and Freundlich) models.

Table 2. Isothermal model parameters for the adsorption of NOR by BB-700.

Models	Parameters	Temperatures (°C)		
		25	35	45
Langmuir	K_a	0.0093	0.0108	0.0074
	Q_{max} (mg/g)	76.1681	77.2239	105.1881
	R^2	0.9679	0.9585	0.9480
Freundlich	K_F	2.7369	3.3342	8.4439
	n	1.7822	1.8896	1.7039
	R^2	0.9355	0.9931	0.9799

The Langmuir isothermal model explains monolayer adsorption on a homogeneous surface, while the Freundlich isothermal model explains multilayer adsorption on a non-homogeneous surface [31]. Our results indicated that the adsorption process of BB-700 for NOR was more consistent with the Langmuir model at 25 °C, with a good fit (R^2 of 0.9679), and the Q_{max} of BB-700 for NOR was 76.1681 mg/g, obtained by the model fitting. However, at 35 and 45 °C, the adsorption of NOR by BB-700 was more consistent with the Freundlich model, and the R^2 values were higher than those from the Langmuir model. Hence, the adsorption of NOR by BB-700 was a monomolecular process at 25 °C, while, at 35 and 45 °C, the adsorption of NOR by BB-700 was a multilayered non-homogeneous physical adsorption process [32]. In addition, as seen in Table 2, the n (1.7882, 1.8896, and 1.7039) was >1 at the three temperatures; this indicated that the adsorption of NOR by BB-700 was favorable at the three temperatures [30]. The maximum theoretical adsorption capacities of BB-700 for NOR at 25, 35, and 45 °C were obtained from the Langmuir isothermal model fitting as 76.1681, 77.2239, and 105.1881 mg/g, respectively.

Adsorption kinetics elucidates the connection between the diffusion process and the contact time of NOR at the solid–liquid interface. This helps to explore the reaction pathways and adsorption mechanisms of the BB [3]. The experimental data of the adsorption kinetics and two model fitting curves are displayed in Figure 6. During the first 60 min, the adsorption rate was faster and the increase in the adsorption capacity was larger because of the abundance on the surface of BB-700 of free active sites that are capable of effectively adsorbing NOR. As the adsorption reaction continued, the adsorption speed decreased while the adsorption capacity increased slowly until the adsorption equilibrium

was reached. The above results may be due to the following reasons: in the initial stage, NOR molecules quickly occupied the empty adsorption site on the surface of BB-700, but over time, the limited adsorption site was occupied by NOR, the adsorption rate slowed down, the adsorption capacity reached the maximum, and the adsorption equilibrium was reached. The kinetic parameters fitted by two kinetics models are displayed in Table 3. By comparing the nonlinear correlation coefficient, it can be observed that the results fitted by the pseudo-second-order model were better than those fitted by the pseudo-first-order under the three concentrations, indicating that the rate of adsorption of NOR by BB-700 is likely to be decided by chemical reaction, or by electron sharing or translocation, among the functional groups of BB-700 and NOR [33]. It can be seen from Table 3, at 20, 50, and 100 mg/L, that the adsorption rate constants of BB-700 were 0.0419, 0.0246, and 0.0155, respectively. As the initial concentration increased, the adsorption rate constant decreased, so that, at the higher initial concentration, much more time was required to achieve the adsorption equilibrium [3].

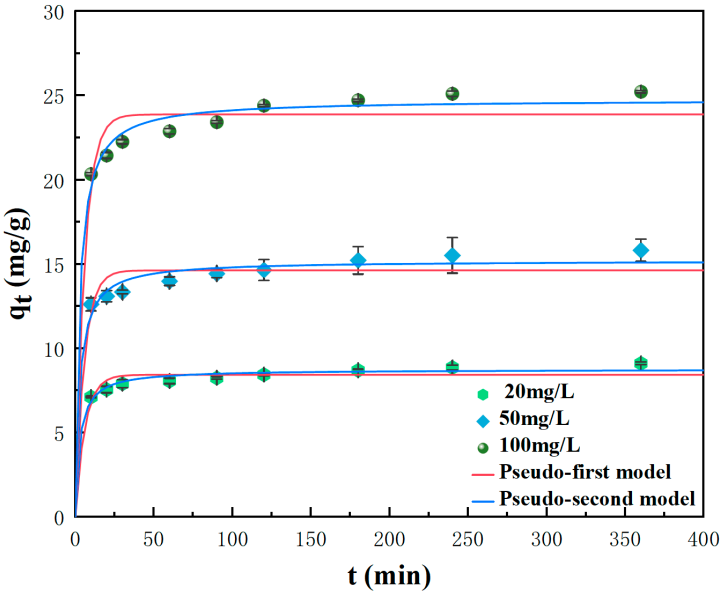

Figure 6. The experimental data and the fitted curves of kinetic models.

Table 3. Kinetic model parameters for the adsorption of NOR by BB-700.

Models	Parameters	Concentrations (mg/L)		
		20	50	100
Pseudo-first-order	k_1	0.1673	0.1769	0.1719
	q_e (mg/g)	8.4439	14.6351	23.8837
	R^2	0.5351	0.4114	0.5344
Pseudo-second-order	k_2	0.0419	0.0246	0.0155
	q_e (mg/g)	8.7616	15.2113	24.7588
	R^2	0.8487	0.7858	0.8729

3.4. Effects of the Ionic Strength and Used in Different Types of Water

The ionic composition of actual wastewater is complicated and variable. The presence of electrolytes will affect the interaction of the biochar and pollutants, necessitating further study of the effects of ion types on NOR adsorption. Since Ca^{2+} and Na^{+} ions are widely present in different water sources, they were selected for this study. The effects of Ca^{2+} and Na^{+} on the NOR adsorption by BB-700 are displayed in Figure 7a,b. As the ionic strength increased, the adsorption capability decreased. The NOR removal rate of BB-700 in Ca^{2+} (from 50.74% to 59.81%) was less than that in Na^{+} (from 67.43% to 82.04%) at the same ionic concentration. The Ca^{2+} and Na^{+} exhibited an inhibitory effect on the adsorption

performance of BB-700 on NOR, which could be explained by the fact that Ca^{2+} and Na^{+} took up the sites on the BB-700 surface. In addition, high concentrations of Ca^{2+} and Na^{+} may have an impact on the electrostatic interactions between BB-700 and NOR ions. The impact of Ca^{2+} on NOR adsorption was more pronounced than that of Na^{+}. This can be ascribed to the higher charge strength of Ca^{2+}, making it more prone to form chelates with surface functional groups on the biochar. In addition, Ca^{2+} could limit the hydrophobic interaction between BB-700 and NOR [30].

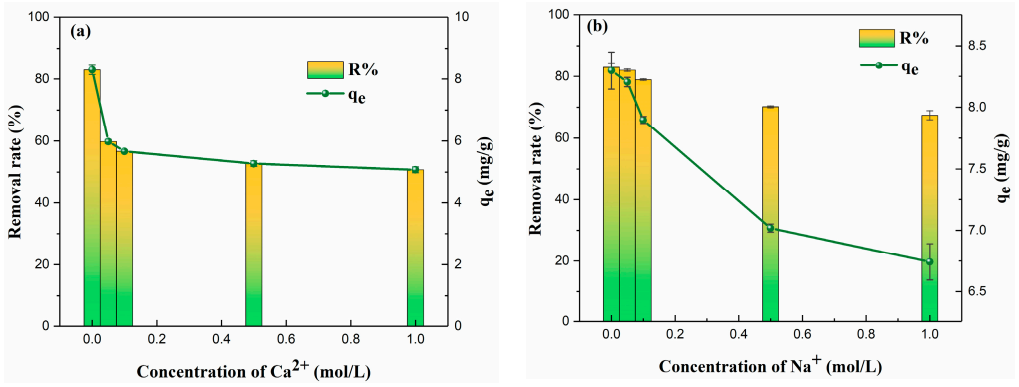

Figure 7. NOR adsorption by BB-700 under the effects of different ionic strengths: (**a**) Ca^{2+}; (**b**) Na^{+}.

The influence of different water types on NOR adsorption by BB-700 is illustrated in Figure 8. Of the three water bodies, tap water was the most affected. This may be because the residual chlorine contained in tap water negatively affects the adsorption effect, followed by river water and pure water, findings that differed from the result of Nguyen et al. [34]. This may be explained by the fact that certain impurities in river water can promote the adsorption of NOR by biochar, which can provide directions for future research. The above results demonstrated that BB-700 can be used to adsorb antibiotics in different water bodies, which provides technical assistance for the practical application of BB-700.

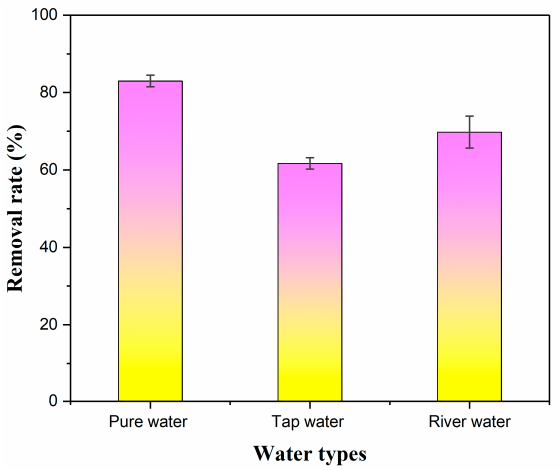

Figure 8. NOR adsorption by BB-700 in different water types.

3.5. Characterization of BB-700

To further explore the adsorption mechanism of BB-700 on NOR, SEM was implemented to characterize the morphology of BB-700. Different-magnification images are shown in Figure 9, and all images show that the surface of BB-700 contains a great number of varied micropores, which may form more active sites that are conducive to NOR adsorption by biochar [6,34].

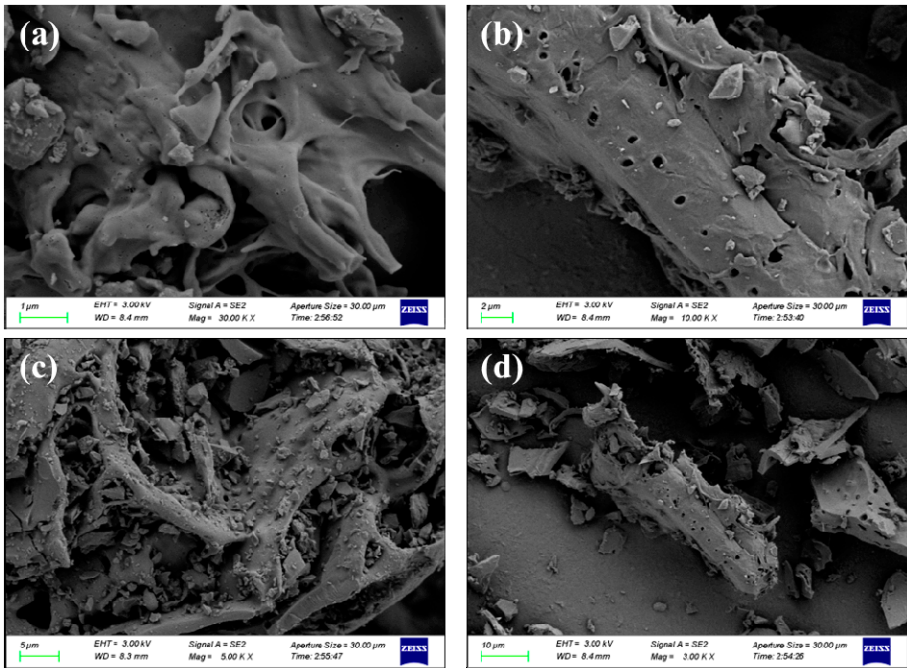

Figure 9. Different magnifications of SEM images of BB-700 (**a**–**d** represents sizes 1, 2, 5, 10 μm, respectively).

Biochar contains surface oxygen-containing functional groups (including carboxyl and hydroxyl groups) that greatly enhance its adsorption of NOR. These groups of biochar are known to greatly impact its adsorption properties on NOR through hydrogen bonding and π–π interactions [35]. The surface functional groups of BB-700 before and after the adsorption of NOR, determined by FTIR, are displayed in Figure 10. The band at 3445 cm^{-1} is caused by the overlap of N-H and O-H groups [36]. The bands near 1613 cm^{-1} indicate the stretching vibrations of C=O and C=C groups [37], and the C-C bond vibrations peak at 667 cm^{-1}, while peaks at 2351 cm^{-1} are probably the adsorption peak of CO_2. As indicated in Figure 10, after adsorption, the peaks at 3445, 2613, and 667 cm^{-1} were obviously changed, which suggests that the surface of BB-700 may have adsorbed NOR. Indeed, the existence of the relative abundance of organic functional groups may promote NOR adsorption on biochar surfaces [38].

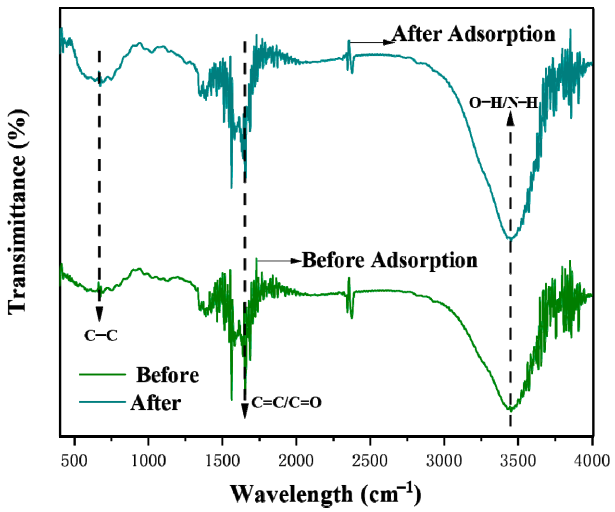

Figure 10. FTIR spectra of BB-700 before and after NOR adsorption.

Figure 11 shows the XRD spectra of BB-700 before and after NOR adsorption. There are two wide peaks of BB-700 between 20–30° and 40–50°, which correspond to the crystalline surface of the amorphous carbon, indicating that BB-700 was transformed from an organo–crystalline compound to a microcrystalline carbon with a finer-grained graphitization structure after carbonization [39,40]. The XRD spectra of BB-700 after the adsorption of NOR are very similar to those of BB-700 before adsorption, except that the intensity decreased. In addition, the XRD spectra of BB-700 after the adsorption of NOR are smoother than before adsorption.

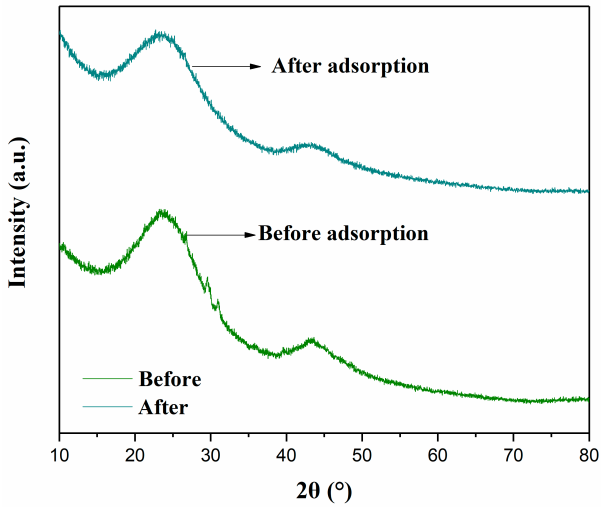

Figure 11. XRD spectra of BB-700 before and after NOR adsorption.

3.6. Comparison of the NOR Adsorption Properties of Other Biomass

To further demonstrate the adsorption performance of BB-700 on NOR, seven other biomass materials were collected to prepare biochars under the same conditions as BB-700. Biochars were derived from different biomass materials: rice straw, wheat straw, soybean straw, corn stalk, rape straw, peanut shell, and *Eichhornia crassipes*. A comparison of the NOR removal effect of the other adsorption materials is displayed in Table 4.

Table 4. Comparison of the NOR removal effect with other adsorption materials.

Biochar	Removal Rate (%)	Adsorption Capacity (mg/g)	Preparation Conditions	Adsorption Conditions
BB-700	99.71	13.29	700 °C, 2 h, 5 °C/min	15 mg biochar, 10 mg/L NOR, 20 mL solutions, 180 min, 150 rpm/min
Peanut shell	88.07	11.74		
Rape straw	89.91	11.99		
Wheat straw	80.63	10.75		
Corn stalk	86.05	11.47		
Rice straw	93.82	12.51		
Soybean straw	85.67	11.42		
Eichhornia crassipes	74.13	9.88		

It can be seen from Table 4 that, under the same adsorption conditions, BB-700 had the best NOR removal efficiency among the biochars prepared from eight different biomass raw materials in the laboratory, with a removal rate of 99.72%, followed by rice straw biochar, with a removal rate of 93.83%. Of all the raw biomass materials, the removal effect of *Eichhornia crassipes* biochar was the worst. From the above results, it can be seen that agroforestry wastes can be feedback for biochar to adsorb antibiotics, which provides technical support for the resource utilization of agroforestry wastes.

3.7. Assumptions and Limitations

Utilizing BB-700 to remediate antibiotic pollution in actual water bodies requires further investigation. Firstly, the long-term environmental risks associated with BB-700 cannot be ignored and necessitate evaluation post-application. Secondly, the impact of dissolved organic matter in water bodies on antibiotic adsorption warrants additional study. When removing antibiotics from tap water and river water, we assume that the organic matter in the water does not affect the adsorption of antibiotics. In fact, on the one hand, organic matter itself will adsorb antibiotics, while on the other hand, organic matter will result in the breeding of microorganisms and the growth of aquatic animals and plants, which will reduce the antibiotic content. Thirdly, in terms of analytical methods, we only used Langmuir and Freundlich models, as well as pseudo-first-order and pseudo-second-order equations, etc., to analyze the adsorption process of biochar more comprehensively, and the van Hoff equation [41] can be considered to further study the thermodynamic properties, and the index (k_2, q_e) can be compared to describe the adsorption kinetics, of the prepared biochar [42]. These are important directions for further research.

4. Conclusions

In this research, biochar was generated from disposable bamboo chopsticks to remove NOR. BB-700 emerged as an excellent adsorbent for the removal of antibiotics from water due to its expansive specific surface area, well-developed pore structure, and notable adsorption capacity. The isotherm and kinetic data suggest that the adsorption of NOR on BB-700 follows a monolayer chemisorption process. The primary adsorption mechanisms involve pore filling, hydrogen bonding, and π–π conjugation. Moreover, BB-700 exhibited robust removal capabilities even in the presence of high concentrations of Na^+ and Ca^{2+} ions. The straightforward preparation method and the high removal efficiency of bamboo-based biochar highlight its potential as a cost-effective adsorbent for environmental remediation.

Author Contributions: Conceptualization, R.Z. and M.Z.; methodology, S.S. and P.L.; validation, S.S. and R.Z.; writing—original draft preparation, R.Z.; writing—review and editing, P.L. and M.Z.; visualization, S.S.; funding acquisition, R.Z. and M.Z. All authors have read and agreed to the published version of the manuscript.

Funding: This research was funded by the Anhui Provincial Natural Science Foundation (Grant Nos. 2008085ME159, 2208085QE176, 2108085QB54), the Key Project of the University Natural Science Research Project of Anhui Province (Grant No. KJ2021A0505), and the Science and Technology Project of Wuhu City (Grant No. 2022jc15).

Data Availability Statement: The raw data supporting the conclusion of this article will be made available by the authors, without undue reservation.

Acknowledgments: We want to acknowledge the journal editors and anonymous reviewers for their valuable comments.

Conflicts of Interest: The authors declare no conflict of interest.

References

1. Wu, Y.; Cheng, H.; Pan, D.; Zhang, L.; Li, W.; Song, Y.; Bian, Y.; Jiang, X.; Han, J. Potassium hydroxide-modified algae-based biochar for the removal of sulfamethoxazole: Sorption performance and mechanisms. *J. Environ. Manag.* **2021**, *293*, 112912. [CrossRef] [PubMed]
2. Nie, Y.; Zhao, C.W.; Zhou, Z.Y.; Kong, Y.L.; Ma, J.Y. Hydrochloric acid-modified fungi-microalgae biochar for adsorption of tetracycline hydrochloride: Performance and mechanism. *Bioresour. Technol.* **2023**, *383*, 129224. [CrossRef] [PubMed]
3. Zhou, H.J.; Wang, Z.; Gao, C.L.; Sun, Q.Q.; Liu, J.; She, D. Synthesis of honeycomb lignin-based biochar and its high-efficiency adsorption of norfloxacin. *Bioresour. Technol.* **2023**, *369*, 128402. [CrossRef] [PubMed]
4. Wang, K.; Wang, Y.; Zhang, S.; Chen, Y.D.; Wang, R.; Ho, S.H. Tailoring a novel hierarchical cheese-like porous biochar from algae residue to boost sulfathiazole removal. *Environ. Sci. Ecotechnol.* **2022**, *10*, 100168. [CrossRef]
5. Pan, Y.; Dong, J.; Wan, L.; Sun, S.; MacIsaac, H.J.; Drouillard, K.G.; Chang, X. Norfloxacin pollution alters species composition and stability of plankton communities. *J. Hazard. Mater.* **2020**, *385*, 121625. [CrossRef]

6. Liu, C.; Wang, Z.Q.; Hua, S.; Jiao, H.; Chen, Y.L.; Ding, D.H. Sewage sludge derived magnetic biochar effectively activates peroxymonosulfate for the removal of norfloxacin. *Sep. Purif. Technol.* **2023**, *314*, 123674. [CrossRef]
7. Karimnezhad, H.; Navarchian, A.H.; Tavakoli Gheinani, T.; Zinadini, S. Amoxicillin removal by Fe-based nanoparticles immobilized on polyacrylonitrile membrane: Effects of input parameters and optimization by response surface methodology. *Chem. Eng. Process. Process Intensif.* **2020**, *147*, 107785. [CrossRef]
8. Zhao, K.; Kang, S.-X.; Yang, Y.-Y.; Yu, D.-G. Electrospun Functional Nanofiber Membrane for Antibiotic Removal in Water: Review. *Polymers* **2021**, *13*, 226. [CrossRef]
9. Ding, D.; Yang, S.; Chen, L.; Cai, T. Degradation of norfloxacin by CoFe alloy nanoparticles encapsulated in nitrogen doped graphitic carbon (CoFe@N-GC) activated peroxymonosulfate. *Chem. Eng. J.* **2020**, *392*, 123725. [CrossRef]
10. Li, Z.; Wang, J.; Chang, J.; Fu, B.; Wang, H. Insight into advanced oxidation processes for the degradation of fluoroquinolone antibiotics: Removal, mechanism, and influencing factors. *Sci. Total Environ.* **2023**, *857*, 159172. [CrossRef]
11. El Azzouzi, L.; El Aggadi, S.; Ennouhi, M.; Ennouari, A.; Kabbaj, O.K.; Zrineh, A. Removal of the Amoxicillin antibiotic from aqueous matrices by means of an adsorption process using Kaolinite clay. *Sci. Afr.* **2022**, *18*, e01390. [CrossRef]
12. Yan, J.; Zuo, X.; Yang, S.; Chen, R.; Cai, T.; Ding, D. Evaluation of potassium ferrate activated biochar for the simultaneous adsorption of copper and sulfadiazine: Competitive versus synergistic. *J. Hazard. Mater.* **2020**, *424*, 127435. [CrossRef] [PubMed]
13. Feng, C.; Zhang, L.; Zhang, X.; Li, J.; Li, Y.; Peng, Y.; Luo, Y.; Li, R.; Gao, B.; Hamouda, M.A.; et al. Bioassembled MgO-coated tea waste biochar efficiently decontaminates phosphate from water and kitchen waste fermentation liquid. *Biochar* **2023**, *5*, 5–22. [CrossRef]
14. Wang, J.; Zhang, M. Adsorption Characteristics and Mechanism of Bisphenol A by Magnetic Biochar. *Int. J. Environ. Res. Public Health* **2020**, *17*, 1075. [CrossRef] [PubMed]
15. Salihi, E.C.; Wang, J.; Kabacaoglu, G.; Kirkulak, S.; Siller, L. Graphene oxide as a new generation adsorbent for the removal of antibiotics from waters. *Sep. Sci. Technol.* **2021**, *56*, 453–461. [CrossRef]
16. Zhuang, S.; Liu, Y.; Wang, J. Covalent organic frameworks as efffcient adsorbent for sulfamerazine removal from aqueous solution. *J. Hazard. Mater.* **2020**, *383*, 121126. [CrossRef]
17. Zhao, R.; Ma, T.; Zhao, S.; Rong, H.; Tian, Y.; Zhu, G. Uniform and stable immobilization of metal-organic frameworks into chitosan matrix for enhanced tetracycline removal from water. *Chem. Eng. J.* **2020**, *382*, 122893. [CrossRef]
18. Maia, R.A.; Louis, B.; Baudron, S.A. Deep eutectic solvents for the preparation and post-synthetic modification of metal- and covalent organic frameworks. *Cryst. Eng. Comm.* **2021**, *23*, 5016–5032. [CrossRef]
19. Yang, R.; Pan, C.; Song, K.X.; Nam, J.C.; Wu, F.; You, Z.X.; Hao, Z.P.; Li, J.J.; Zhang, Z.S. Bamboo-derived hydrophobic porous graphitized carbon for adsorption of volatile organic compounds. *Chem. Eng. J.* **2023**, *461*, 141979.
20. Hien, T.T.T.; Tsubota, T.; Taniguchi, T.; Shinogi, Y. Enhancing soil water holding capacity and provision of a potassium source via optimization of the pyrolysis of bamboo biochar. *Biochar* **2021**, *3*, 51–61. [CrossRef]
21. Zheng, Q.Y.; Wang, W.J.; Wen, J.; Wu, R.H.; Wu, J.F.; Zhang, W.Y.; Zhang, M.Y. Non-additive effects of bamboo-derived biochar and dicyandiamide on soil greenhouse gas emissions, enzyme activity and bacterial community. *Ind. Crop. Prod.* **2023**, *194*, 116385. [CrossRef]
22. Chen, G.; Viengvilay, K.; Yu, W.; Mao, T. Effect of Different Modification Methods on the Adsorption of Manganese by Biochar from Rice Straw, Coconut Shell, and Bamboo. *ACS Omega* **2023**, *8*, 28467–28474. [CrossRef] [PubMed]
23. Cheng, J.; Bi, C.; Zhou, X.; Wu, D.; Wang, D. Preparation of Bamboo-Based Activated Carbon via Steam Activation for Efficient Methylene Blue Dye Adsorption: Modeling and Mechanism Studies. *Langmuir* **2023**, *39*, 14119–14129. [CrossRef] [PubMed]
24. Huang, J.; Zimmerman, A.R.; Chen, H.; Gao, B. Ball milled biochar effectively removes sulfamethoxazole and sulfapyridine antibiotics from water and wastewater. *Environ. Pollut.* **2020**, *258*, 113809. [CrossRef] [PubMed]
25. Zhou, R.J.; Zhang, M.; Li, J.Y.; Zhao, W. Optimization of preparation conditions for biochar derived from water hyacinth by using response surface methodology (RSM) and its application in Pb^{2+} removal. *J. Environ. Chem. Eng.* **2020**, *8*, 104198. [CrossRef]
26. Atugoda, T.; Gunawardane, C.; Ahmad, M.; Vithanage, M. Mechanistic interaction of ciproffoxacin on zeolite modiffed seaweed (*Sargassum crassifolium*) derived biochar: Kinetics, isotherm and thermodynamics. *Chemosphere* **2021**, *281*, 130676. [CrossRef]
27. Liu, H.; Xu, G.; Li, G. The characteristics of pharmaceutical sludge-derived biochar and its application for the adsorption of tetracycline. *Sci. Total Environ.* **2020**, *747*, 141492. [CrossRef]
28. Quesada, H.B.; Cusioli, L.F.; de O Bezerra, C.; Baptista, A.T.; Nishi, L.; Gomes, R.G.; Bergamasco, R. Acetaminophen adsorption using a low-cost adsorbent prepared from modified residues of *Moringa oleifera* Lam. seed husks. *J. Chem. Technol. Biotechnol.* **2019**, *94*, 3147–3157. [CrossRef]
29. Zelaya, S.M.E.; Flores, F.M.; Torres, S.R.M.; Fernández, M.A. Norfloxacin adsorption on montmorillonite and carbon/montmorillonite hybrids: pH effects on the adsorption mechanism, and column assays. *J. Environ. Sci. Health Part A* **2020**, *56*, 113–122. [CrossRef]
30. Zhang, X.Z.; Zhen, D.W.; Liu, F.M.; Chen, R.; Peng, Q.R.; Wang, Z.Y. An achieved strategy for magnetic biochar for removal of tetracyclines and fluoroquinolones: Adsorption and mechanism studies. *Bioresour. Technol.* **2023**, *369*, 128440. [CrossRef]
31. Priya, S.; Manish, S.; Harshita, L.; Ragini, G.; Madhu, A. Non-toxic and biodegradable κ-carrageenan/ZnO hydrogel for adsorptive removal of norfloxacin: Optimization using response surface methodology. *Int. J. Biol. Macromol.* **2023**, *238*, 124145.

32. Lei, H.; Muhammad, Y.; Wang, K.; Yi, M.; He, C.; Wei, Y.; Fujita, T. Facile fabrication of metakaolin/slag-based zeolite microspheres (M/SZMs) geopolymer for the efficient remediation of Cs^{+} and Sr^{2+} from aqueous media. *J. Hazard. Mater.* **2021**, *406*, 124292. [CrossRef]
33. Li, Y.; Shang, H.; Cao, Y.; Yang, C.; Feng, Y.; Yu, Y. High performance removal of sulfamethoxazole using large specific area of biochar derived from corncob xylose residue. *Biochar* **2022**, *4*, 11. [CrossRef]
34. Chen, Y.; Li, J.; Wang, F.; Yang, H.; Liu, L. Adsorption of tetracyclines onto polyethylene microplastics: A combined study of experiment and molecular dynamics simulation. *Chemosphere* **2021**, *265*, 129133. [CrossRef] [PubMed]
35. Liu, P.; Li, H.; Liu, X.; Wan, Y.; Han, X.; Zou, W. Preparation of magnetic biochar obtained from one-step pyrolysis of salix mongolica and investigation into adsorption behavior of sulfadimidine sodium and norfloxacin in aqueous solution. *J. Dispers. Sci. Technol.* **2020**, *41*, 214–226. [CrossRef]
36. Nguyen, V.T.; Vo, T.D.H.; Nguyen, T.B.; Nguyen, D.D.; Bui, T.H.; Nguyen, X.C.; Tran, T.; Le, T.N.C.; Duong, T.G.H.; Bui, M.H.; et al. Adsorption of norffoxacin from aqueous solution on biochar derived from spent coffee ground: Master variables and response surface method optimized adsorption process. *Chemosphere* **2022**, *288*, 132577. [CrossRef] [PubMed]
37. Wu, J.Q.; Wang, T.S.; Liu, Y.Y.; Tang, W.; Geng, S.Y.; Chen, J.W. Norfloxacin adsorption and subsequent degradation on ball-milling tailored N-doped biochar. *Chemosphere* **2023**, *303*, 135264. [CrossRef]
38. Ashiq, A.; Vithanage, M.; Sarkar, B.; Kumar, M.; Bhatnagar, A.; Khan, E.; Xi, Y.; Ok, Y.S. Carbon-based adsorbents for fluoroquinolone removal from water and wastewater: A critical review. *Environ. Res.* **2021**, *197*, 111091. [CrossRef]
39. Zeng, X.Y.; Wang, Y.; Li, R.X.; Cao, H.L.; Li, Y.F.; Lü, J. Impacts of temperatures and phosphoric-acid modification to the physicochemical properties of biochar for excellent sulfadiazine adsorption. *Biochar* **2022**, *4*, 14. [CrossRef]
40. Yang, F.; Jin, C.; Wang, S.; Wang, Y.J.; Wei, L.; Zheng, L.H.; Gu, H.P.; Lam, S.S.; Naushad, M.; Li, C.; et al. Bamboo-based magnetic activated carbon for efficient removal of sulfadiazine: Application and adsorption mechanism. *Chemosphere* **2023**, *323*, 138245. [CrossRef]
41. Kooh, M.R.R.; Dahri, M.K. Removal of methyl violet 2B dye from aqueous solution using Nepenthes rafflesiana pitcher and leaves. *Appl. Water. Sci.* **2017**, *7*, 3859–3868. [CrossRef]
42. Wu, F.; Tseng, R.L.; Huang, S.C.; Juang, R.S. Characteristics of pseudo-second-order kinetic model for liquid-phase adsorption: A mini-review. *Chem. Eng. J.* **2009**, *151*, 1–9. [CrossRef]